MOF-Graphite Oxide Composites: Combining the Uniqueness of Graphene Layers and Framework of MOF

By *Camille Petit*, and *Teresa J. Bandosz**

[*] Camille Petit. Corresponding author: Teresa J. Bandosz.
Department of Chemistry
The City College and the Graduate School of the City University of New York
160 Convent Avenue
New York, NY 10031 (USA)
E-mail: tbandosz@ccny.cuny.edu

Keywords: metal-organic framework, graphite oxide, nanocomposite, adsorbent, porosity.

Abstract

Graphite oxide (GO) / metal-organic framework (MOF-5) nanocomposites are synthesized with various ratios of the two components. In developing the concept of these new adsorbents, it was expected that distorted graphene sheets would contribute to the enhancement in the dispersive interactions, whereas MOF-5 component would contribute to the expansion of the pore space where adsorbates could be stored. Moreover, taking into account the variety of transition and noble metals, which can be used to form the MOF structure, those materials have a potential to provide active sites for reactive adsorption or heterogeneous catalysis. The composites have a unique layered sandwich-like structure where GO units divide the MOF-5 units. A possible scenario for the formation of such structures is the involvement of linkages between epoxy groups of distorted graphene layers of GO and zinc oxide building units of MOF-5. An increase in the content of GO leads to a greater distortion of the MOF-5 cubic structure and visible changes in the texture of nanocomposites. The materials are predominantly microporous with sizes of pores defined by the cavities of MOF-5 units. Moreover, specific combination and synergy between GO and MOF-5 units also result in the formation of a unique porosity characteristic of the nanocomposites.

Introduction

Recently a great interest rose in the scientific community in graphene and graphene-based materials.[1-3] It is owing to the specific and very unique structural, mechanical, and electronic properties of those one-atom-thin sheets. The common source of graphene is graphite, which can be considered as three-dimensional crystals consisting of graphene layers. Separation of graphite into graphene layers is not a trivial task and many attempts have been made based on graphite oxide (GO). GO is formed by treating graphite with very strong oxidizing agents[4] and has a layered structure and a non-stoichiometric chemical composition. It has been used recently to build various nanocomposites which exhibit enhanced electronic and adsorption properties.[5-10] The graphene layers of GO are stacked together with an interlayer distance varying from 6-12 Å depending on the level of hydration.[11] Oxidation of graphite causes introduction of epoxy and hydroxyl groups to the graphene layers, as well as carboxylic groups mainly located on the edges of the layers.[12, 13] Moreover, strong oxidation also leads to defects in the layers in the form of incorporated oxygen atoms or vacancies.[14, 15] This increase in hydrophilicity causes that GO is easily dispersed in water and delaminated in alkaline media or alcohols.[12, 16] Then the graphite layers can be restacked and their degree of orientation depends on the method of drying.

Another group of materials which has recently open new possibilities of applications are Metal-Organic Frameworks (MOFs).[17, 18] Yaghi and coworkers were the first group describing their synthesis and properties.[19-21] During recent years it has been shown that a large variety of 2-D and 3-D metal organic networks with high porosity, unusual ions exchange and adsorptive properties can be designed using intermolecular interactions and metal-ligand coordination.[22-25] The structure of the materials obtained is the result of

maximum degrees of freedom of both components, spherical shape of metal ions and well-defined points of contacts in the organic linkers.[26]

In spite of the very high porosities of MOFs, their open framework is not able to provide strong nonspecific adsorption forces to retain small molecules at ambient conditions. For this kind of separation processes, a surface consisting of a dense arrangement of atoms and porous network is needed. An ideal situation is when that dense surface creates an accessible porous framework with pores similar in sizes to the target molecule. This is not an easy task and for years various methods of sorbent synthesis and modifications have been explored to provide the best suitable surface features.

To meet the above mentioned requirements in adsorption processes, the concept of graphite oxide-MOF nanocomposite has been developed in our laboratory. Knowing the ratios of GO and MOF in the composites, it is expected that distorted graphene sheets will contribute to the enhancement in the dispersive interactions, whereas MOF component will contribute to the expansion of the pore space where the adsorbate can be stored. Moreover, taking into account the variety of transition and noble metals which can be used to form the MOF structure, those materials have a potential to provide active sites for reactive adsorption or heterogeneous catalysis. There are also other unforeseen applications where the presence of graphene can increase the electrical conductivity of the resulting materials.

Examples of metal organic frameworks are MOF-n materials which are built from the extended analogues of molecular metal-carboxylate clusters.[20] They are stable at rather high temperature and their porosity can reach 60 %.[22] The preparation of MOFs involves reaction between solutions of metal ions salts and organic linkers. Besides, as mentioned above, a

broad range of transition or noble metals can be used in the synthesis owing to their catalytic properties.[27]

Thus a major objective of this paper is to present the synthesis of MOF-GO nanocomposite materials, which combine the favorable attributes of carbonaceous graphene surfaces and MOFs. As a metal-organic framework, MOF-5 was chosen for this study, owing to its relatively small sizes of pores (~ 8 Å) and the chemistry of the linkages. In MOF-5, $[Zn_4O]^{6+}$ tetrahedra form the corners of the resulting primitive cubic structure, while benzene carboxylates (1,4 benzenedicarboxylate, BDC) allow the junction between these zinc oxide clusters.[28] The formula of the resulting material is $Zn_4O(H\text{-}BDC)_3$.[22] Since epoxy and carboxylic groups are present on GO, it is expected that they might anchor zinc oxide clusters. Synthesis of the parent materials and the nanocomposites is followed by their surface characterization using a range of experimental methods. The different nanocomposites consisting in 5, 10 and 20 wt % of graphite oxide are presented. To our best knowledge, the synthesis of such materials has not been reported in the literature. We characterize the new materials from the point of view of their structure, texture and porosity. The nanocomposites are referred to as MOF-5-GO1, MOF-5-GO2 and MOF-5-GO3 where 1, 2 and 3 represent the 5, 10 and 20 wt % of GO in the samples, respectively.

Results and discussion

Since in our materials MOF-5 represents the major component of the nanocomposites, one would expect a predominance of MOF-5 structure features on the X-ray diffraction patterns of the nanocomposites. Of course, it should only happen when MOF-5 synthesis in the presence of GO does no prevent the formation of linkages between the zinc oxide and BDC. In fact, in our concept of composite formation, we envisioned the formation of small units of MOF-5,

which would be linked to the distorted graphene sheets owing to the presence of epoxy groups present on the graphene sheets or carboxylic groups located at the edges.[12-15] The former scenario would be more favorable for the formation of layered composites. As seen in **Fig. 1**, the major diffraction pattern of MOF-5 is preserved in our composites and this pattern is in agreement with those previously reported for MOF-5.[29, 30] For GO, the peak at 2 Theta about 9.29 ^{o} represents the interlayer distance of 9.5 Å.[31] For MOF-5-GOn (n = 1, 2 or 3) nanocomposites, the sharpness of the peak at 2 Theta about 9.7 ^{o} is slightly reduced and the splitting of that peak is noticed. This splitting increases in its visibility with an increase in the content of GO. A similar feature was observed by Lillerud and coworkers on MOF-5. They attributed it to a distortion of the cubic symmetry.[30] Finding it for our composites indicates that the presence of GO in the sample increases the distortion in the MOF-5 cubic arrangement. One could expect such an effect since there are additional constraints in the degrees of freedom during synthesis caused by the presence of GO, and they increase with an increase in the content of GO. Other interesting features, quite unique for MOF-5-GO composites, are sharp peaks between 2 Theta 30 and 40 ^{o}. They are much less sharp for MOF-5 and almost not present for MOF-5-GO2. Thus they must represent differences in the building units of MOF-5-GO2 and the two other composites.

The texture of the nanocomposites can be observed on SEM micrographs presented in **Fig. 2**. For comparison, micrographs for GO and MOF-5 are also included. In the latter sample, the cubic crystals of MOF-5 are clearly visible with some traces of amorphous phase. GO is seen as dense agglomerates/flakes of graphene sheets stacked together by dispersive forces. On the other hand, the agglomerates of MOF-5-GO1 nanocomposite look totally different. They consist of regular square-shaped thin platelets of about 500 x 50 nm stacked together in an organized way. Taking into account the differences in the texture between MOF-5-GO1, MOF-5 and GO, it is plausible to assume that thin agglomerates of graphene layers act as

dividers located between the thin platelets of MOF-5. This leads to the formation of that sandwich-like structure. For MOF-5-GO2, although some indication of the layered structure can be seen, the edges of the platelets are much less sharp. It is likely that more GO interfere with the MOF-5 crystallization pattern. Those changes are even more visible for MOF-5-GO3 where 20 wt % GO is present. Owing to the pronounced differences in the densities of both components in MOF-5-GO3, the physical contact of both phases must be extended and MOF-5 crystallizes as about 50 nm in diameter worm-like structures connected to the edges on graphene platelets. The EDAX element maps of the nanocomposites are presented in the supporting information. They show that carbon, oxygen and zinc are well-dispersed on the surface, which suggests that for all composites, GO and MOF-5 interact to form new materials of homogenous structure and chemistry. Taking into account the chemistries of both components of nanocomposites, we hypothesized the building process of the ordered structure of MOF-5-GO1. A schematic and simplified version of the mechanism is proposed in **Fig. 3.** In a first step, MOF-5 "blocks" attach to a graphene layer by reactions with epoxy groups on GO. This can happen similarly to water interactions with MOF-5, as analyzed by Greathouse and Allendorf.[32] According to them, a replacement of an oxygen atom in ZnO_4 tetrahedron by oxygen atom from water is a very important step leading to the decomposition of MOF-5 by water. In our case, we assume that oxygen atoms in epoxy groups on GO play the same role as oxygen atoms in water. However, no collapse of MOF-5 structure occurs owing to the limitations in the number of epoxy groups and their restricted spatial location compared to free molecules of water. Hydrogen bonding between hydrogen atom from hydroxyl groups on GO and oxygen atoms in ZnO_4 tetrahedron might increase the degree of interaction between graphene layers and MOF-5 crystal. Hydrogen bonding between water molecules and ZnO_4 tetrahedron was also described by Greathouse and Allendorf.[32] In the subsequent steps of the nanocomposite building process, an alternation between attachment of graphene layers and MOF-5 "blocks" happens. The mechanism of the structure formation might be different for

MOF-5-GO3. In this sample, more GO is present than for the other two composites and consequently the amount of carboxylic groups on the edges of the layers is higher. Those groups must have a greater affinity for zinc oxide tetrahedron than epoxy groups have. Attachment of MOF-5 "blocks" on the edges of the GO layers might accompany the above described mechanism or be a preferred mechanism, leading to the formation of worm-like structures as seen in SEM images (**Fig. 2F)**

The textural homogeneity is reflected on nitrogen adsorption isotherms presented in **Fig. 4**. They have well-defined Langmuir-type shape indicating microporosity and pores of uniform sizes, which is in agreement with the structural model of cavities in MOF-5 in which the passage of spheres of diameter up to 8.0 Å have been defined.[28] From these isotherms, the parameters of porous structure were calculated. They are collected in Table 1. In this Table, we also report the hypothetical values of the surface areas and pore volumes assuming the physical mixture of the components. We report the surface area only for the sake of comparison however for such materials as MOFs, having an open framework, reporting the pore volume seems to be more appropriate because fewer assumptions are used for its calculation. GO, as reported previously,[33] is nonporous from the point of view of nitrogen used as a molecular probe. It is important to notice that the surface area of MOF-5 is smaller than 3000-3500 $m^2.g^{-1}$ reported elsewhere.[20, 29] Nevertheless, surfaces of similar magnitude were reported by Huang and coworkers, and Panella and coworkers.[34, 35] The difference in the surface area can be related to the way of outgassing during preparation and thus the completeness of solvent removal. Other factors such as the temperature at which crystals were formed were also indicated as potentially affecting the porosity.[29, 36]

The composites have a high volume of micropores and less than 10% total pore volume in mesopores. The latter increases with an increase in the content of GO. The most developed

porosity is found for MOF-5-GO2 which is an interesting finding since its texture, as seen from SEM micrograph, is considered as ”in between” the ones for the samples formed from 5 and 20 wt % of GO. Apparently 10 wt % GO results in the most porous materials with about 12 % increase in the parameters of the porous structure compared to the porosity of the hypothetical physical mixture of the components. For the other two materials, especially for MOF-5-GO3, the measured volume of micropores is less than the hypothetical one. This can be related to the distortion in the MOF-5 cubic arrangement which was observed on X-ray diffraction. This was also reflected in the texture of the composite. The lack of the well-defined trend in the porosity of the composites can be the result of the small differences in the synthesis conditions. Although the maximum in the porosity is expected based on the properties of GO and MOF-5, investigation only three composites does not allow us to indicate the specific composition leading to the most developed porosity.

Conclusions

To conclude, nanocomposites containing graphite oxide and metal-organic framework (MOF-5) have been prepared with various ratios of the two components. The structure of the precursors is preserved in the composites. The latter ones show a well-defined and porous structure where graphene layers from GO alternate with layers of MOF-5. The arrangement of these materials is progressively modified and its porosity decreased when the amount of GO in the composite increases. It is hypothesized that the formation of such structure occurs via interactions between epoxy groups from graphene layers and zinc oxide clusters from MOF-5. Due to their preserved porosity and well-developed and flexible functionality, these materials might be tested for gas adsorption applications.

Experimental

Materials

Graphite oxide was synthesized by oxidation of graphite (Sigma-Aldrich) using the Hummers' method [37]. Briefly, graphite powder (10 g) was stirred with cool concentrated sulfuric acid (230 mL at 0 ^{o}C). Then, potassium permanganate (30 g) was added to the suspension slowly to prevent a rapid rise in temperature (less than 20 ^{o}C). The reaction mixture was then cooled to 2 ^{o}C. After removal of the ice-bath, the mixture was stirred at room temperature for 30 min. Distilled water (230 mL) was slowly added to the reaction vessel to keep the temperature under 98 ^{o}C. The diluted suspension was stirred for an additional 15 min and further diluted with distilled water (1.4 L), before adding hydrogen peroxide (100 mL). The mixture was left overnight. GO particles, settled at the bottom, were separated from the excess liquid by decantation followed by centrifugation. The remaining suspension was transferred to dialysis tubes (MW cutoff 6,000-9,000). Dialysis was carried out until no precipitate of $BaSO_4$ was detected by addition of $BaCl_2$. Then, the wet form of graphite oxide was centrifuged and freeze-dried. A fine brown powder of the initial graphite oxide was obtained. The resulting material is referred to as GO.

MOF-5 was prepared by mixing zinc nitrate hexahydrate (10.4 g) and 1,4 benzenedicarboxylate (2 g) in N,N dimethylformamide (DMF, 140 mL) until complete dissolution of the solids. Then, the mixture was transferred into a round flask connected to a condenser and heated at 115-120 ^{o}C for 24 hours. After cooling, the supernate was removed and crystals deposited on the bottom of the flask were collected, washed with DMF, and immersed in fresh chloroform overnight. Chloroform was changed twice during two days. Finally, crystals were collected, placed inside a closed filtering flask connected to an aspirator used to create vacuum inside the flask, and heated at 130-135 ^{o}C for six hours. The resulting crystals were then kept in a dessicator.

The composite materials were prepared by dispersing GO powder in the well-dissolved zinc nitrate/BDC mixture. The resulting suspensions were subsequently stirred and subjected to the same synthesis procedure as for MOF-5. The added GO consists of 5 wt %, 10 wt % or 20

wt % weight final material. The synthesized composites are referred to as MOF-5-GO1, MOF-5-GO2 and MOF-5-GO3, respectively.

Textural characterization

Textural characterization was carried out by measuring the N_2 adsorption isotherms at –196 ^oC. Before the experiments, the samples were outgassed under vacuum at 120 ^oC. The isotherms were used to calculate the specific surface area, S_{BET}, total pore volume, V_{tot} volume of micropores, V_{mic}, volume of mesopores, V_{mes}, and pore size distributions. The volume of pores, and surface in pores larger than 10 Å were obtained using density functional theory (DFT) [38].

Electron microscopy (SEM/EDAX)

Scanning electron microscopy was performed on a Zeiss Supra 55 instrument. The instrument has a resolution of 5 nm at 30 kV. Scanning was performed on a sample powder previously dried and sputter coated with a thin layer of carbon to avoid charging. EDAX analyses were done on the same instrument with samples previously dried and coated with gold and palladium (to avoid charging and allow carbon content determination more accurately). From EDAX analyses, the content of elements on the surface was calculated and the maps of the elements derived.

X-ray diffraction

X-ray diffraction (XRD) measurements were conducted using standard powder diffraction procedures. Adsorbents were ground with DMF in a small agate mortar. The mixture was smear-mounted onto a glass slide and then analyzed by Cu K_α radiation generated in a Philips X'Pert X-ray diffractometer. A standard glass slide was run for the background correction.

Acknowledgments
This work was supported by the ARO (Army research office) grant W911NF-05-1-0537 and the NSF Collaborative grant 0754945/0754979.
Supporting Information is available online from Wiley InterScience.

Received: ((will be filled in by the editorial staff))
Revised: ((will be filled in by the editorial staff))
Published online: ((will be filled in by the editorial staff))

[1] S. Stankovich, D. A. Dikin, G. H. B. Dommett, K. M. Kohlhaas, E. J. Zimney, E. A. Stach, R. D. Piner, S. B. T. Nguyen, R. S. Ruoff, *Nature* **2006**, *442*, 282.

[2] D. A. Dikin, S. Stankovich, E. J. Zimney, R. D. Piner, G. H. B. Dommett, G. Evmenenko, S. B. T. Nguyen, R. S. Ruoff, *Nature* **2007**, *448*, 457.

[3] S. Stankovich, D. A. Dikin, R. D. Piner, K. A. Kohlhaas, A. Kleinhammes, Y. Jia, Y. Wu, S. B. T. Nguyen, R. S. Ruoff, *Carbon* **2007**, *45*, 1558.

[4] Brodie, B. C. *Ann. Chim. Phys.* **1860**, *59*, 466.

[5] Z.-H. Liu, Z.-M. Wang, X. Yang, K. Ooi, *Langmuir* **2002**, *18*, 4926.

[6] X. Yang, Y. Makita, Z.-H. Liu, K. Ooi, *Chem. Mater.* **2003**, *15*, 1228.

[7] J. Li, L. Vaisman, G. Marom, J.-K. Kim, *Carbon* **2007**, *45*, 744.

[8] Z.-M. Wang, K. Shishibori, K. Hoshinoo, H. Kanoh, T. Hirotsu, *Carbon* **2006**, *44*, 2479.

[9] M. Seredych, A. V. Tamashausky, T. J. Bandosz, *Carbon* **2008**, *46*, 1241.

[10] C. Petit, T. J. Bandosz, *J. Phys. Chem. C* **2009**, *113*, 3800.

[11] A. Buchsteiner, A. Lerf, J. Pieper, *J. Phys. Chem. B* **2006**, *110*, 22328.

[12] T. Szabo, E. Tombacz, E. Illes, I. Dekany, *Carbon* **2006**, *44*, 537.

[13] Lerf, A.; He, H.; Forster, M.; Klinowski, J. *J. Phys. Chem. B* **1998**,*102*, 4477.

[14] J. L. Li, K. N. Kudin, M. J. McAllister, R. K. Prud'homme, I. A. Aksay, R. Car, *Phys. Rev. Lett.* **2006**, *96*, 176101.

[15] A. Hashimoto, K. Suenaga, A. Gloter, K. Urita, S. Iijima, *Nature* **2004**, *430*, 870.

[16] M. Hirata, T. Gotou, S, Horiuchi, M. Fujiwara, M, Ohba, *Carbon* **2004**, *42*, 2929.

[17] J. L.C. Rowsell, O. M. Yaghi, *Microporous Mesoporous Mater.* **2004**, *73*, 3.

[18] M. J. Rosseinsky, *Microporous Mesoporous Mater.* **2004**, *73*, 15.

[19] O. M. Yaghi, H. Li, *J. Am. Chem. Soc.* **1995**, *117*, 10401.

[20] M. Eddaoudi, H. Li, O. M. Yaghi, *J. Am. Chem. Soc.* **2000**, *122*, 1391.

[21] J. Kim, B. Chen, T. M. Reineke, H. Li, M. Eddaoudi, D. M. Moler, M. O'Keeffe, O. M. Yaghi, *J. Am. Chem. Soc.* **2001**, *123*, 8239.

[22] M. Eddaoudi, J. Kim, N. Rosi, D. Vodak, J. Wachter, M. O'Keeffe, O. M. Yaghi, *Science* **2002**, *295*, 469.

[23] D. Britt, D. Tranchemontagne, O. M. Yaghi, *Proc. Nat. Acad. Sci. U.S.A.* **2008**, *105*, 11623.

[24] B. Chen, S. Ma, E. J. Hurtado, E. B. Lobkovsky, C. Liang, H. Zhu, S. Dai, *Inorg. Chem.* **2007**, *46*, 8705.

[25] D. Y. Siberio-Perez, A. G. Wong-Foy, O. M. Yaghi, A. J. Matzger, *Chem. Mater.* **2007**, *19*, 3681.

[26] J. Kim, B. Chen, T. M. Reineke, H. Li, M. Eddaoudi, D. B. Moler, M. O'Keeffe, O. M. Yaghi, *J. Am. Chem. Soc.* **2001**, *123*, 8239.

[27] J. Hafizovic, A. Krivokapic, K. C. Szeto, S. Jakobsen, K. P. Lillerud, U. Olsbye, M. Tilset, *Cryst. Growth Des.* **2007**, *7*, 2302.

[28] H. Li, M. Eddaoudi, M. O'Keeffe, O. M. Yaghi, *Nature* **1999**, *402*, 276.

[29] S. S. Kaye, A. Dailly, O. M. Yaghi, J. R. Long, *J. Am. Chem. Soc.* **2007**, *129*, 14176.

[30] J. Hafizovic, M. Bjørgen, U. Olsbye, P. D. C. Dietzel, S. Bordiga, C. Prestipino, C. Lamberti, K. P. Lillerud, *J. Am. Chem. Soc.* **2007**, *129*, 3612.

[31] C. Hontoria-Lucas, A. J. Lopez-Peinado, J. de D. Lopez-Gonzalez, M. L. Rojas-Cervantes, R. M. Martin-Aranda, *Carbon* **1995**, *33*, 1585.

[32] J. A. Greathouse, M. D. Allendorf, *J. Am. Chem. Soc.* **2006**, *120*, 10678.

[33] M. Seredych, C. Petit, A. V. Tamashausky, T. J. Bandosz, *Carbon* **2009**, *47*, 445.

[34] L. Huang, H. Wang, J. Chen, Z. Wang, J. Sun, D. Zhao, Y. Yan, *Microporous Mesoporous Mater.* **2003**, *58*, 105.

[35] B. Panella, M. Hirscher, *Adv. Mater.* **2005**, *17*, 538.

[36] U. Mueller, M. Schubert, F. Teich, H. Puetter, K. Schierle-Arndt, J. Pastre, *J. Mater. Chem.* **2006**, *16*, 626.

[37] W. S. Hummers, R. E. Offeman, *J. Am. Chem. Soc.* **1958**, *80*, 1339.

[38] C. M. Lastoskie, K. E. Gubbins, N. Quirke, *J. Phys. Chem*. **1993**, *97*, 4786.

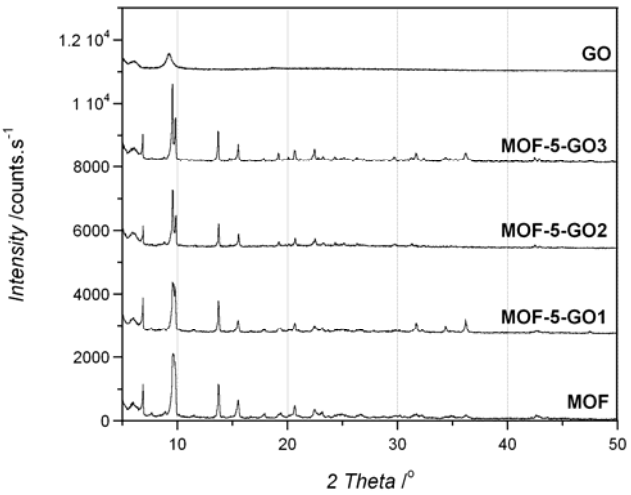


Figure 1. X-ray diffraction patterns for the parent materials and the composites.

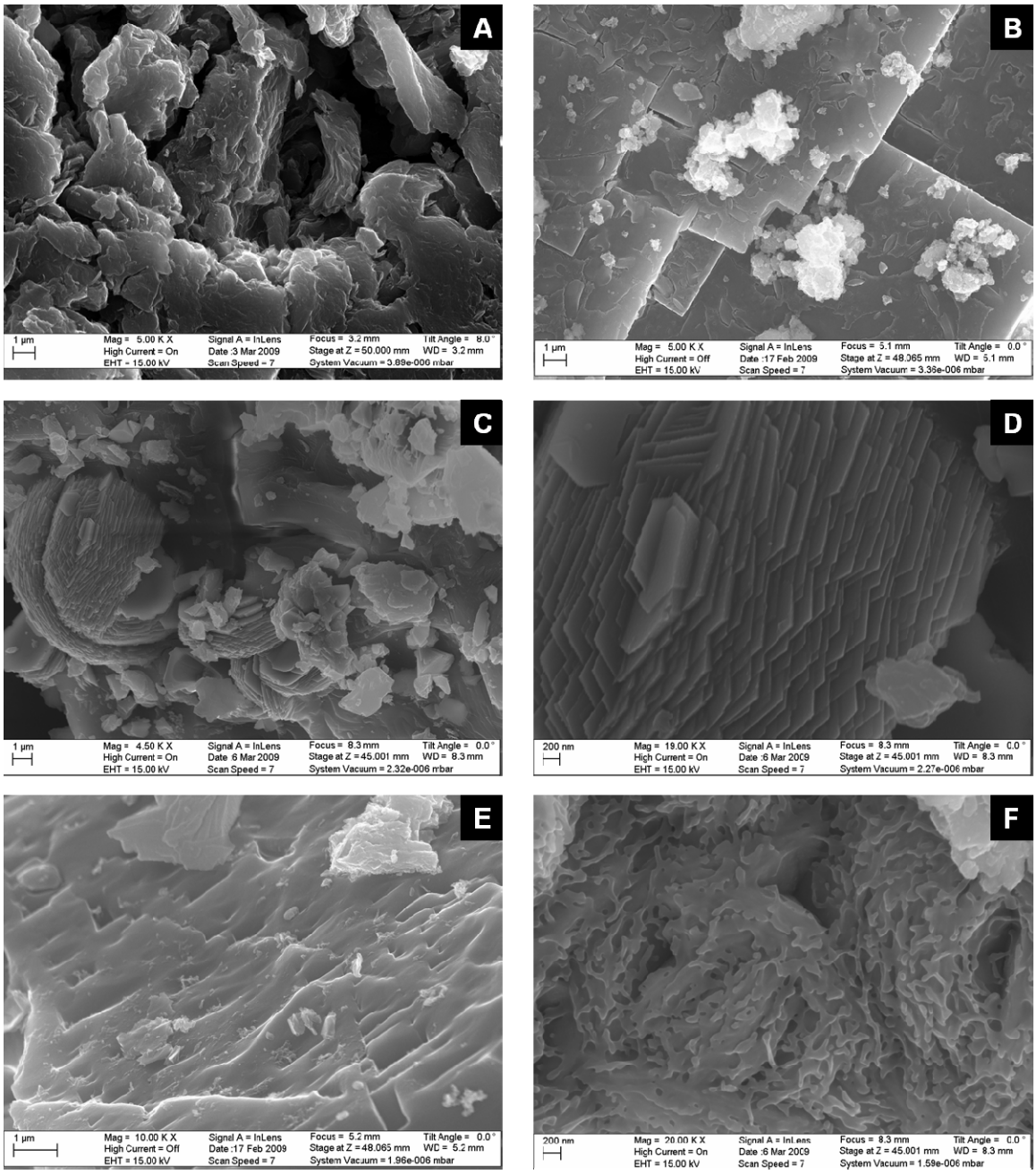


Figure 2. SEM micrographs for the parent materials and the composites. (A): GO, (B): MOF-5, (C): MOF-5-GO1, (D) MOF-5-GO1, (E): MOF-5-GO2 and (F): MOF-5-GO3.

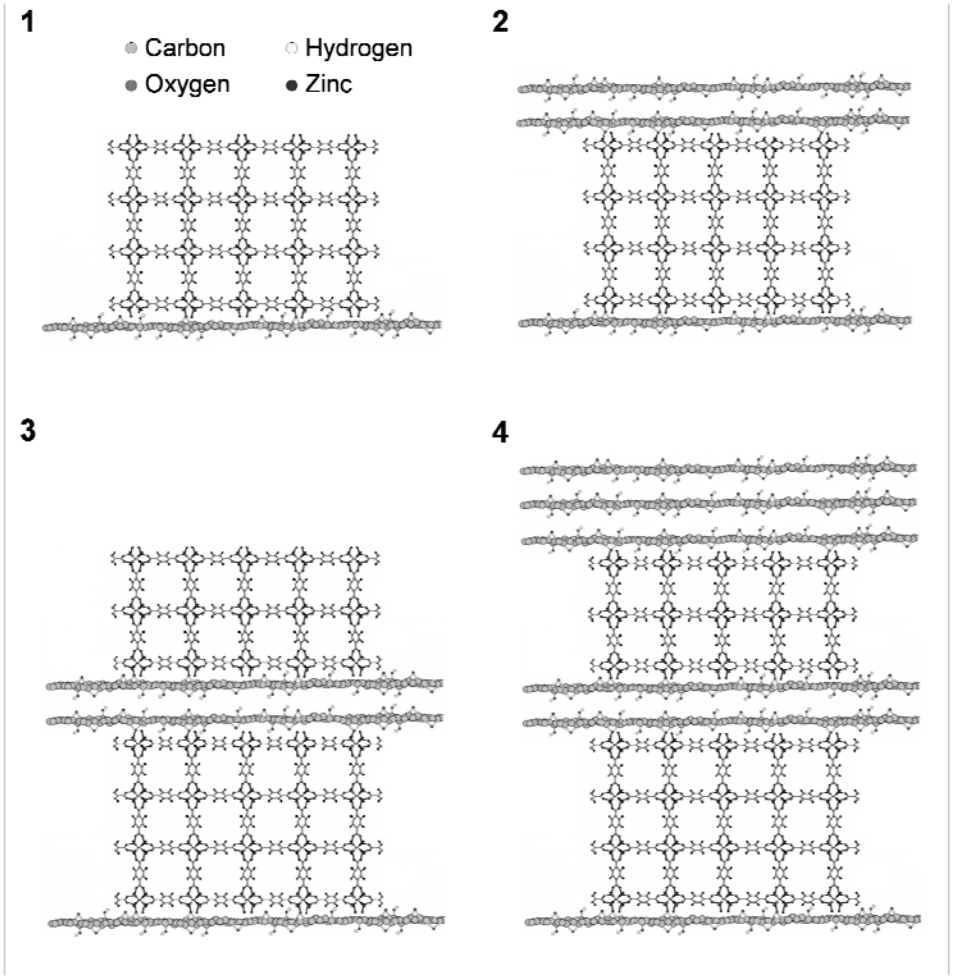


Figure 3. Schematic view of the steps (1-4) of the nanocomposite (MOF-5-GO1) formation. In black: C atoms in MOF-5, in green: C atoms in GO, in blue: Zn atoms, in red: O atoms, in grey: H atoms.

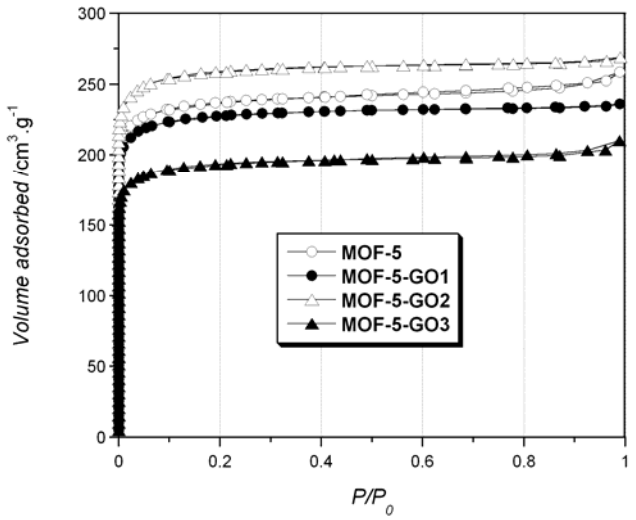


Figure 4. Nitrogen adsorption isotherms for the parent materials and the composites.

Table 1. Parameters of porous structure calculated from adsorption of nitrogen and hypothetical values (H) derived assuming the physical mixture of the nanocomposite components.

Sample	S_{BET} [$m^2.g^{-1}$]	V_{tot} [$cm^3.g^{-1}$]	V_{meso} [$cm^3.g^{-1}$]	V_{mic} [$cm^3.g^{-1}$]	$S_{BET}H$ [$m^2.g^{-1}$]	V_{tot} H [$cm^3.g^{-1}$]	V_{mic} H [$cm^3.g^{-1}$]
GO	nil	nil	nil	nil	-	-	-
MOF-5	793	0.408	0.023	0.385	-	-	-
MOF-5-GO1	706	0.365	0.024	0.341	753	0.388	0.366
MOF-5-GO2	806	0.416	0.028	0.388	714	0.367	0.347
MOF-5-GO3	603	0.325	0.037	0.288	634	0.327	0.308

Table of contents

Nanocomposites containing graphite oxide (GO) and metal-organic framework (MOF) are prepared. They have a well-defined structure where graphene layers from GO alternate with layers of MOF, via linkages between epoxy groups from GO and zinc oxide from MOF. The enhanced porosity and dispersive forces of the composites compared to the precursors provide views for applications in gas adsorption.

Keyword: composite material, metal-organic framework.

C. Petit, T. J. Bandosz*

MOF-Graphite Oxide Composites: Combining the Uniqueness of Graphene Layers and Framework of MOF

